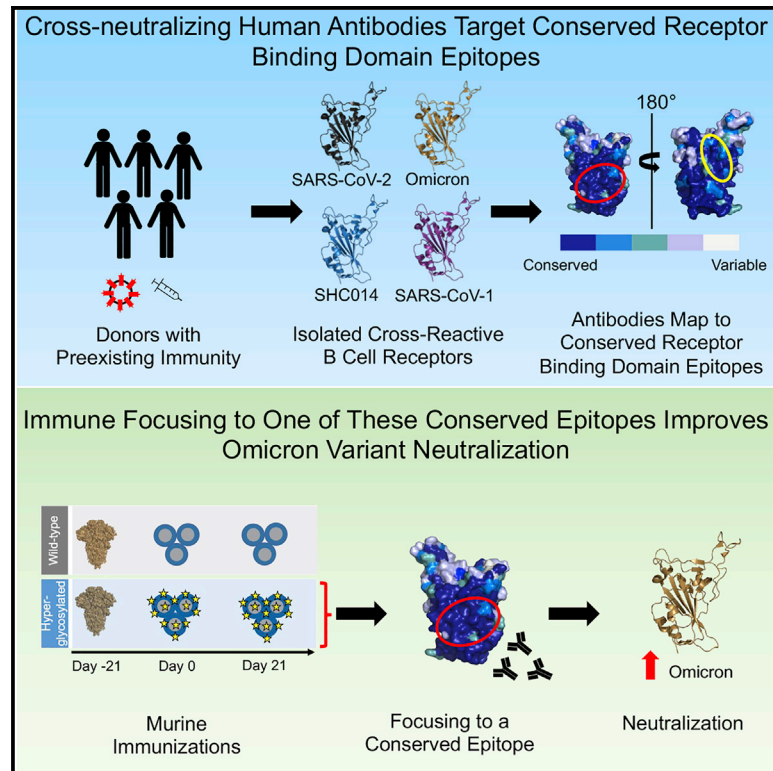


Cross-reactive SARS-CoV-2 epitope targeted across donors informs immunogen design

Graphical abstract



Authors

Blake M. Hauser, Jared Feldman, Maya Sangesland, ..., Daniel Lingwood, Wilfredo F. Garcia-Beltran, Aaron G. Schmidt

Correspondence

aschmidt@crystal.harvard.edu

In brief

Hauser et al. characterize human antibodies elicited by SARS-CoV-2 vaccination or infection that bind broadly to different sarbecovirus receptor-binding domains. Broadly cross-neutralizing antibodies target two conserved epitopes. Structure-guided immunogen design focuses murine antibody responses to one such epitope in the context of pre-existing immunity, conferring improved Omicron neutralization.

Highlights

- Broad sarbecovirus reactivity exists in the human RBD-directed antibody repertoire
- Broadly cross-neutralizing antibodies predominantly target two conserved epitopes
- A rationally designed immunogen focuses responses to one conserved epitope
- Immune-focused murine antibody responses confer improved Omicron neutralization



Report

Cross-reactive SARS-CoV-2 epitope targeted across donors informs immunogen design

Blake M. Hauser,¹ Jared Feldman,¹ Maya Sangesland,¹ Larance Ronsard,¹ Kerri J. St. Denis,¹ Maegan L. Sheehan,¹ Yi Cao,¹ Julie Boucau,¹ Ian W. Windsor,^{1,2,3,4} Agnes H. Cheng,¹ Mya L. Vu,¹ Marcella R. Cardoso,¹ Ty Kannegieter,¹ Alejandro B. Balazs,¹ Daniel Lingwood,¹ Wilfredo F. Garcia-Beltran,^{1,5} and Aaron G. Schmidt^{1,2,6,*}

¹Ragon Institute of MGH, MIT and Harvard, Cambridge, MA 02139, USA

²Department of Microbiology, Harvard Medical School, Boston, MA 02115, USA

³Department of Biological Chemistry and Molecular Pharmacology, Harvard Medical School, Boston, MA 02115, USA

⁴Laboratory of Molecular Medicine, Boston Children's Hospital, Boston, MA 02115, USA

⁵Department of Pathology, Massachusetts General Hospital, Boston, MA 02114, USA

⁶Lead contact

*Correspondence: aschmidt@crystal.harvard.edu

<https://doi.org/10.1016/j.xcrm.2022.100834>

SUMMARY

The emergence of the antigenically distinct and highly transmissible Omicron variant highlights the possibility of severe acute respiratory syndrome coronavirus 2 (SARS-CoV-2) immune escape due to viral evolution. This continued evolution, along with the possible introduction of new sarbecoviruses from zoonotic reservoirs, may evade host immunity elicited by current SARS-CoV-2 vaccines. Identifying cross-reactive antibodies and defining their epitope(s) can provide templates for rational immunogen design strategies for next-generation vaccines. Here, we characterize the receptor-binding-domain-directed, cross-reactive humoral repertoire across 10 human vaccinated donors. We identify cross-reactive antibodies from diverse gene rearrangements targeting two conserved receptor-binding domain epitopes. An engineered immunogen enriches antibody responses to one of these conserved epitopes in mice with pre-existing SARS-CoV-2 immunity; elicited responses neutralize SARS-CoV-2, variants, and related sarbecoviruses. These data show how immune focusing to a conserved epitope targeted by human cross-reactive antibodies may guide pan-sarbecovirus vaccine development, providing a template for identifying such epitopes and translating to immunogen design.

INTRODUCTION

As severe acute respiratory syndrome coronavirus 2 (SARS-CoV-2) continues to evolve because of population immunity, antigenically distinct variants such as Omicron may emerge.¹ This antigenic difference increases the likelihood that there will be re-infections or breakthrough infections following vaccination.^{1–8} Furthermore, surveillance efforts have identified related sarbecoviruses in animal reservoirs that use the human ACE2 receptor for viral entry, suggesting possible future pandemics.^{9–12} Consequently, there is a need for cross-reactive therapeutic antibodies or next-generation vaccines that protect against SARS-CoV-2 variants and novel sarbecoviruses with pandemic potential. While many SARS-CoV-2 therapeutic monoclonal antibodies developed early in the pandemic had reduced potency against Omicron, boosting with mRNA vaccines appeared to improve serum neutralization against this and other variants.^{4,13–15} Identifying infection- or vaccine-elicited cross-reactive antibodies can inform immunogen design efforts that focus responses to conserved epitopes.

Here, we analyzed 10 donors from a previous cohort that had serum neutralization against SARS-CoV-2 variant pseudovi-

rus⁴ to characterize cross-reactive memory B cells to additional variants and pre-emergent sarbecoviruses (Table S1). All donors had at least three documented exposures to SARS-CoV-2: 5 received two SARS-CoV-2 vaccines and had at least one SARS-CoV-2 infection, and 5 had three mRNA vaccinations and no known prior SARS-CoV-2 infection. Serum from each donor neutralized wild-type SARS-CoV-2, Delta, Omicron, and SARS-CoV-1 pseudoviruses⁴ (Table S1). Neutralization was significantly reduced against Omicron and SARS-CoV-1 relative to wild-type SARS-CoV-2; neutralization of SARS-CoV-1 was also significantly reduced relative to Delta.

RESULTS

Cross-reactive memory B cell repertoire

We characterized the cross-reactive memory B cell repertoire targeting wild-type SARS-CoV-2, Omicron, and related sarbecoviruses SARS-CoV-1 and SHC014; these represent genetically diverse coronavirus clade members that use human ACE2 for viral entry.¹⁶ We isolated quadruple cross-reactive class-switched (swIg) B cells targeting the wild-type SARS-CoV-2, Omicron, SARS-CoV-1, and SHC014 receptor-binding domains



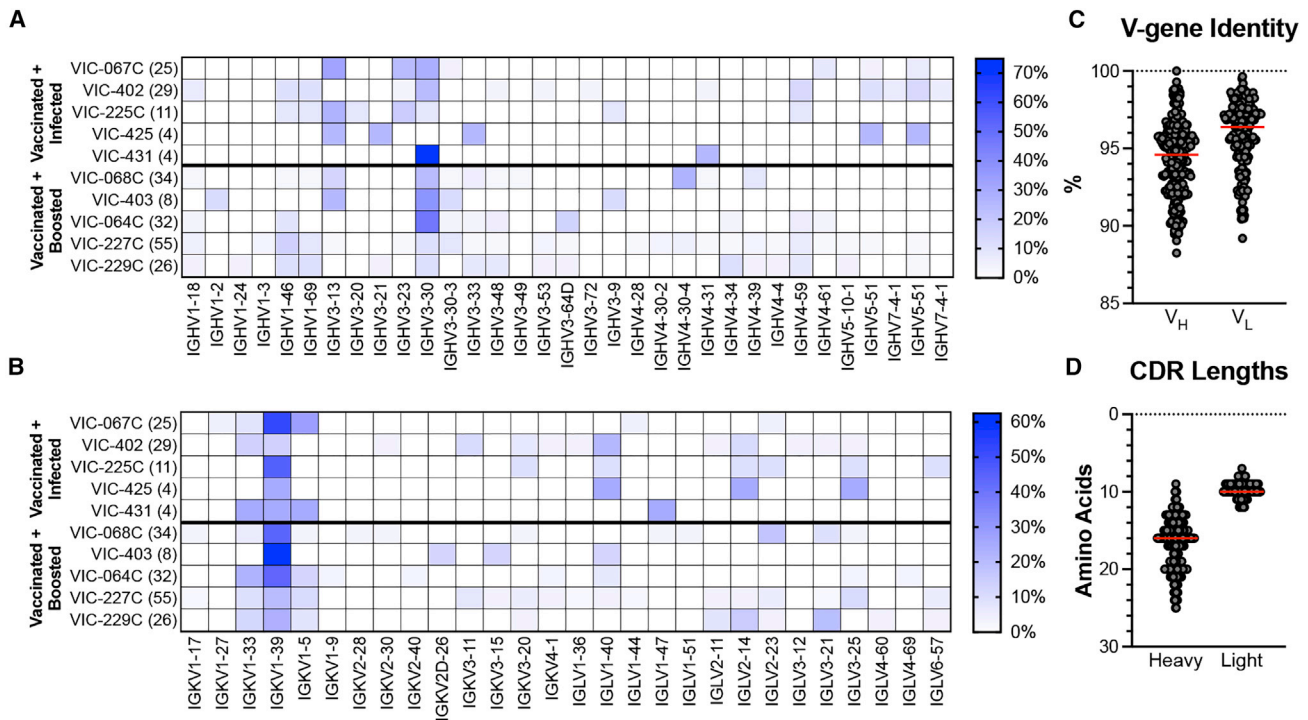


Figure 1. Genetic properties of isolated class-switched B cells

(A and B) Isolated B cells were sequenced, and (A) heavy- and (B) light-chain V-gene usage was characterized. Shading indicates percentage of B cells isolated from a given donor with a given V-gene. Donors in the top half are the vaccinated and infected cohort, while donors in the bottom half are the vaccinated and boosted cohort. Numbers in parentheses are total sequences.

(C) Percentage of V-gene identity to germline was determined for variable heavy (V_H) and variable light (V_L) chains of the 228 sequenced B cell receptors; red line denotes median.

(D) CDR lengths in amino acids for V_H and V_L chains of the 228 sequenced B cells; red line denotes median (related to Figures S1 and S2).

(RBDs) (Figures S1A–S1C). We found that of swlg B cells, a median of 0.3% (interquartile range [IQR] 0.2%–0.8%) bound both wild-type SARS-CoV-2 and Omicron RBDs (Figure S2A). Of those cross-reactive B cells, a median of ~35% (IQR 27%–43%) cross-reacted with both SARS-CoV-1 and SHC014 RBDs (Figure S2B).

We obtained paired heavy- and light-chain sequences for 228 wild-type SARS-CoV-2⁺/Omicron⁺/SARS-CoV-1⁺/SHC014⁺ RBD quadruple cross-reactive class-switched B cells from 10 donors. While 33 different IGHV genes were used across 57 different alleles (Figures 1A and S2C), IGHV3-30 was the most frequently used gene, consistent with observations from other RBD-directed B cells from convalescent patients with SARS-CoV-2.^{17–19} However, the distribution of IGHV gene usage varied from wild-type SARS-CoV-2 RBD-specific memory B cells as reported previously, with less frequent usage of several genes including IGHV3-53, 1–46, 3–23, 3–9, and 1–69.^{17–19} This suggests that a majority of wild-type SARS-CoV-2 RBD-specific B cell receptors may target non-conserved epitopes. IGKV1-39, 1–33, and 1–5 were the most prevalent genes (Figures 1B and S2D). V-gene usage did not vary significantly between donors who were vaccinated and infected versus donors who were vaccinated and boosted. The median V-gene germline identity was ~95% (IQR 92%–96%) for heavy chains and ~96% (IQR 95%–98%) for light chains (Figure 1C). The median CDRH3

length was ~16 amino acids (IQR 14–20), and the median CDRL3 length was ~10 amino acids (IQR 9–10) (Figure 1D).

Mapping cross-reactive antibody epitopes

We next selected 29 paired heavy and light chains that reflected the genetic diversity of the 228 sequenced B cell receptors (BCRs) for recombinant expression as immunoglobulin G (IgG) for further biochemical characterization. Recombinant antibodies were first tested in an ELISA for binding to wild-type SARS-CoV-2, Omicron, SARS-CoV-1, and SHC014 RBDs (Figure 2A). Twenty antibodies had high-affinity binding ($K_D < 1 \mu\text{M}$) to all four RBDs, ranging from <0.1 to 200 nM affinity; 4 antibodies bound all RBDs except Omicron, and 5 bound to two or fewer RBDs.

We down-selected 19 antibodies from 5 donors (Table S2) based on expression levels for epitope mapping by cross-competition ELISA using the wild-type SARS-CoV-2 RBD (Figure 2B). We included control antibodies with structurally defined epitopes: B38 (class 1), P2B-2F6 (class 2), S309 (class 3), CR3022 (class 4), and ADI-55688 (precursor to broadly neutralizing therapeutic antibody ADG-2).^{16,20–24} While several antibodies competed with ACE2 receptor-binding motif (RBM)-directed antibodies B38, P2B-2F6, or ADI-55688, most cross-reactive antibodies mapped to two distinct epitopes. One class competed with CR3022 (class 4), while the other class showed no competition with any control antibodies in ELISA. To define the targeted epitope, we chose

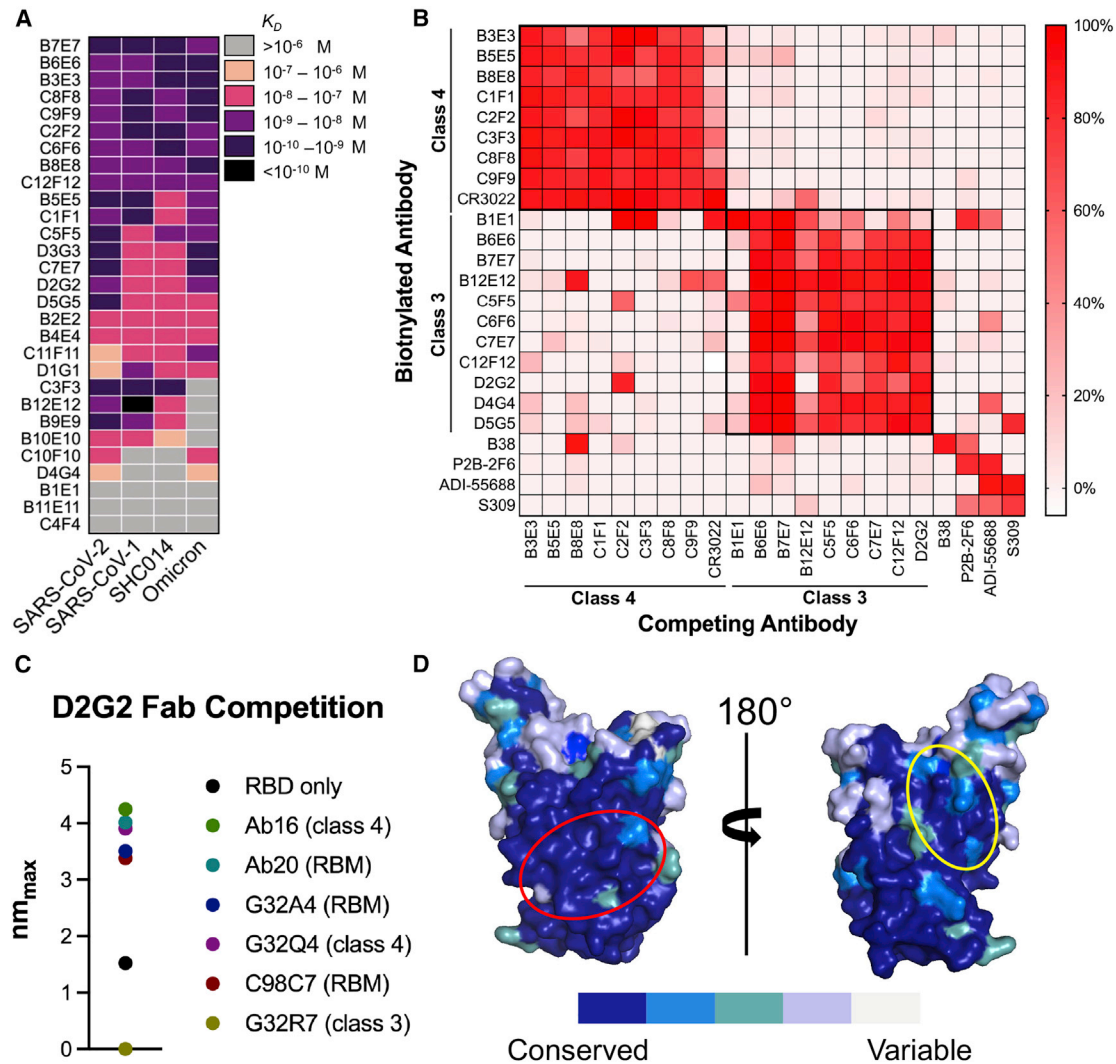


Figure 2. Biochemical characterization of recombinant IgGs

(A) Twenty-nine antibodies were down-selected from sorted swlg B cells for recombinant IgGs expression and assayed for binding to SARS-CoV-2, SARS-CoV-1, SHC014, and Omicron RBDs by single-replicate standard-curve-generating ELISA.

(B) IgG competition targeting different epitope classes²⁰ assayed by ELISA; darker coloring indicates a higher degree of competition averaged over three technical replicates. Antibodies D4G4 and D5G5 were only used as competitor antibodies. Class 3- and 4-targeted antibodies are defined. Control antibody epitopes mapped onto the SARS-CoV-2 RBD (PDB: 6M0J).

(C) Antibody competition with D2G2 (a representative of the group of antibodies that does not target a class 4 epitope) was assessed via BLI. SARS-CoV-2 RBD at 8 μ M was complexed with at least a 5-molar excess of Fab for 30 min, and then binding of the complex to D2G2 Fab was measured via standard single-replicate BLI. Ni-NTA sensors were used with D2G2 immobilized and complexes as the analytes. Max absorbance (nm) for each sample is shown.

(D) Surface conservation across the SARS-CoV-2 wild-type, Omicron, SHC014, and SARS-CoV-1 RBDs (PDB: 6M0J). Circles indicate the approximate footprint of the class 4 (red) and class 3 (yellow) broadly neutralizing human antibodies identified in this study.

representative antibody D2G2 and assayed for competition using biolayer interferometry (BLI) with an additional panel of structurally characterized Fabs: two from mice that represent distinct RBD epitopes, Ab20 and Ab16,²⁵ and four from human donors targeting minimally overlapping RBM and non-RBM epitopes on the RBD, G32A4, C98C7, G32R7, and G32Q4²⁶ (Figure 2C). Only G32R7 competed with D2G2, indicating that the other class of broadly cross-reactive antibodies targets a conserved class 3 epitope that minimally competes with S309, strongly suggesting that the epitope is across that face of the RBD^{20,26–28} (Figure 2D). Of the

11 class 3-directed antibodies characterized, 8 used IGHJ4; only 2 of the 8 class 4-directed antibodies used IGHJ4 (Table S2). There were no other clear patterns of antibody sequence features associated with either of the conserved epitopes, suggesting multiple evolutionary pathways that converge on these conserved epitopes. Broadly reactive antibodies have been previously shown to target both class 3 and 4 epitopes;^{27,29} the lack of class 1 and 2 antibodies characterized here indicates that broadly reactive antibodies targeting these epitopes are less represented in the human memory repertoire.^{30,31}

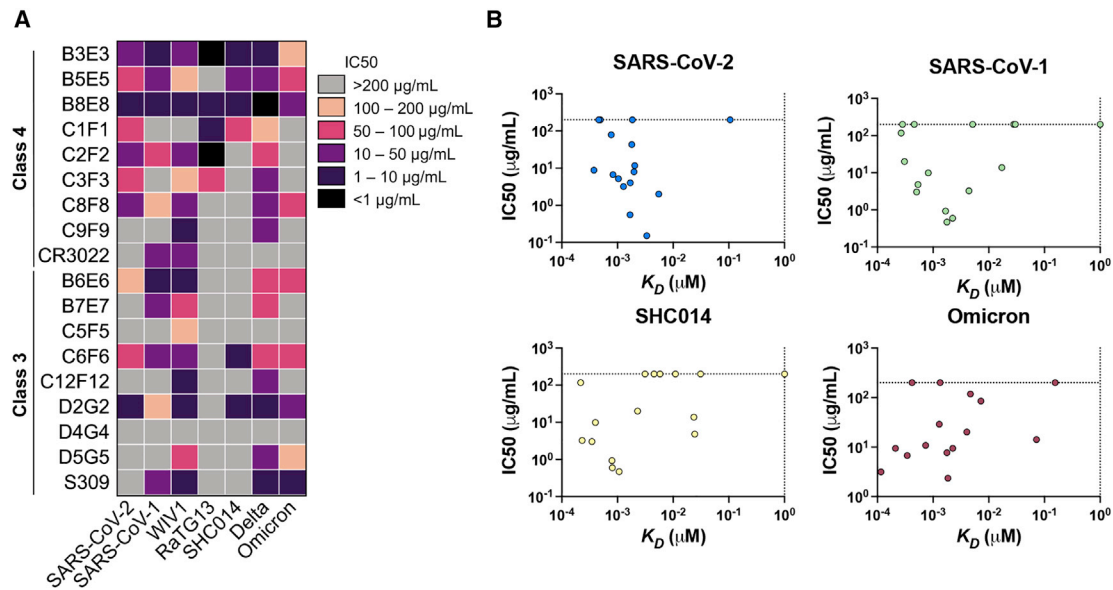


Figure 3. Pseudovirus neutralization of broadly cross-reactive antibodies

(A) Pseudovirus neutralization performed with two technical replicates for 19 antibodies selected for cross-competition, as well as CR3022 (class 4) and S309 (class 3) controls. Antibodies are grouped based on target epitope. IC50s were determined via non-linear curve fits. Results for antibodies with no detectable neutralization are not shown.

(B) Comparison between pseudovirus neutralization as shown in (A) and antibody binding affinity as shown in Figure 2A for four sarbecoviruses (related to Figure S3).

Cross-reactive antibody neutralization

We next performed pseudovirus neutralization assays on the 19 antibodies down-selected for cross-competition against wild-type SARS-CoV-2, SARS-CoV-1, WIV1, RaTG13, SHC014, and the SARS-CoV-2 variants Delta and Omicron. Representative antibodies targeting the two conserved epitopes based on competition were broadly neutralizing with IC50s ranging from ~1 to 200 μg/mL in a pattern that roughly correlated with antibody affinity (Figures 3A and 3B). Seven antibodies targeting the class 4 conserved epitope and 3 antibodies targeting the class 3 conserved epitope neutralized at least 4 of the 7 pseudoviruses tested (though none of the class 3 antibodies neutralized RaTG13). These data indicate that cross-reactive antibodies elicited by vaccination or infection that target both sites are broadly neutralizing antibodies. We also tested antibodies against authentic wild-type SARS-CoV-2 and Omicron and found preserved neutralization (Figure S3).

An engineered immunogen for epitope targeting

Based on these observations across human donors, we used a structure-guided approach to design an immunogen to focus antibody responses to the class 4 epitope. Using glycan engineering, we developed a hyperglycosylated immunogen that selectively exposed this epitope while occluding all other epitopes (Figures 4A, S4A, and S4B); this builds upon our previous hyperglycosylated immunogens to direct immune responses to conserved epitopes.²⁵ This class 4-focusing immunogen has 11 engineered putative N-linked glycosylation sites; 9 are novel and two are native to SARS-CoV-2. We made trimeric versions of this immunogen using a non-immunogenic, hyperglycosylated GCN4 trimerization

tag to increase valency and for subsequent testing *in vivo*²⁵ (Figures S4C–S4F). Two murine cohorts were primed with the SARS-CoV-2 spike to approximate pre-existing vaccine or infection-elicited immunity to SARS-CoV-2 followed by boosting with trimeric wild-type SARS-CoV-2 RBD (“WT cohort”) or the hyperglycosylated immunogen (“HG cohort”) (Figure 4B).

Assessing immunogenicity and focusing

We assayed sera binding 14 days after the second boost against coronavirus RBDs by ELISA. Both cohorts had similar reactivity to all sarbecovirus RBDs tested, but the WT cohort showed a significant drop off in reactivity against the Omicron RBD versus the SARS-CoV-2 RBD, while the HG cohort did not (Figures S4G–S4H). To assess immune focusing to the class 4 epitope, we assayed competition of the murine class 4 antibody Ab16, which competes with CR3022 but has broad neutralization activity across SARS-CoV-2 variants and other sarbecoviruses.²⁵ Ab16 competes with CR3022 and the class 4 donor antibodies (Figures 4C and S4F), and the Ab16 footprint was previously structurally characterized;²⁵ Ab16 was also used to confirm the conformational integrity of the HG immunogen (Figure S4A). The HG cohort had significant increase in serum competition with Ab16, with a mean serum competition of ~2.5× relative to WT (Figure 4D); this indicates that boosting with the HG immunogen immune focuses to the class 4 epitope.

Immune focusing improves cross-neutralization

We assessed serum pseudovirus neutralization of WT SARS-CoV-2, Delta and Omicron variants, and related sarbecoviruses RaTG13, SARS-CoV-1, WIV1, and SHC014. Sera from all cohorts had broad

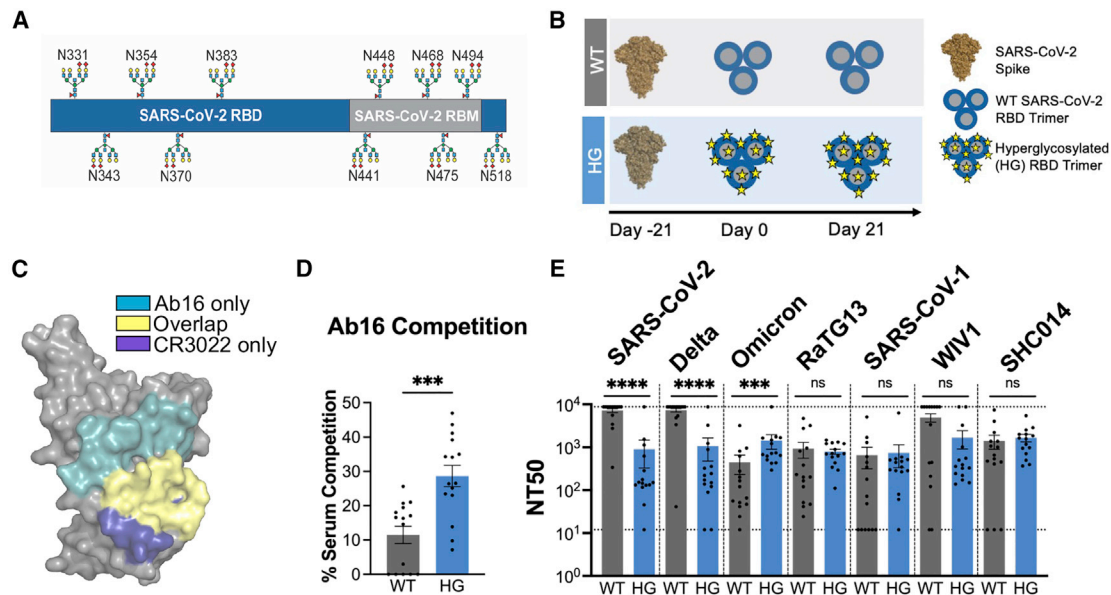


Figure 4. Design, expression, and *in vivo* characterization of a hyperglycosylated class 4-focusing immunogen

(A) Schematic for hyperglycosylated class 4-focusing immunogen; both non- and native-engineered glycans are included (PDB: 6VXX).
 (B) Schematic of immunization cohorts; each cohort contains $n = 15$ total mice. Two separate replicates of this experiment were performed, the first with $n = 5$ mice and the second with $n = 10$ mice.
 (C) Ab16 (teal) and CR3022 (violet) epitopes and overlap (yellow) shown on SARS-CoV-2 RBD (PDB: 6M0J).
 (D) Day 35 serum competition with Ab16 assayed in ELISA coated with SARS-CoV-2 RBD. ELISAs were performed with three technical replicates for each of the $n = 15$ mice.
 (E) Day 35 serum assayed against wild-type SARS-CoV-2, SARS-CoV-2 variants, and related sarbecoviruses for neutralization. Pseudovirus neutralization assays were performed with two technical replicates, and IC50s were determined via non-linear curve fits.
 For (D) and (E), bars represent mean \pm SEM. Statistical significance determined using the Mann-Whitney U test (* $p < 0.05$, ** $p < 0.01$, *** $p < 0.001$, **** $p < 0.0001$, ns, not significant) (related to Figure S4).

neutralization with NT50s ranging from $\sim 10^3$ – 10 against WT SARS-CoV-2 to $\sim 10^2$ – 10^3 against SARS-CoV-1 and WIV1 (Figure 4E). Neutralization of WT SARS-CoV-2 and the closely related Delta variant was significantly lower in the HG cohort; however, neutralization of Omicron was significantly improved in the HG cohort (Figure 4E). Neutralization of related sarbecoviruses RaTG13, SARS-CoV-1, WIV1, and SHC014 showed no significant differences between the WT and HG cohorts (Figure 4E). This is consistent with the fact that there is no significant decrease in the HG cohort between neutralization of WT SARS-CoV-2 and all other coronaviruses tested, while there are significant decreases in the WT cohort (Figures S4I–S4J). Because serum antibody responses from the HG cohort significantly competed with Ab16 (class 4 epitope), relative to the WT cohort (Figure 4D), this suggests that the observed immune focusing elicited by this first-generation immunogen may also neutralize future antigenically distinct SARS-CoV-2 variants. While these data demonstrate a proof-of-principle that focusing SARS-CoV-2 serum antibody responses to a broadly neutralizing epitope can improve breadth, the lack of improved serum neutralization across other sarbecoviruses (Figures S4I–S4J) indicates that further iterative design cycles are necessary.

DISCUSSION

A continued understanding of the nature of the broadly cross-reactive repertoire elicited by SARS-CoV-2 infection and vacci-

nation is necessary given that additional SARS-CoV-2 variants and other related sarbecoviruses will emerge. Characterizing human cross-reactive antibodies may help identify candidate therapeutic monoclonal antibodies that limit the likelihood of viral escape. Currently available monoclonal antibodies were largely selected based on potent WT SARS-CoV-2 neutralization, but Omicron evades neutralization by many of them, particularly those that target epitopes in the RBM (class 1 and 2 epitopes).^{13–15} Emerging SARS-CoV-2 variants or other sarbecoviruses may still escape even broadly cross-reactive antibodies, but identifying multiple antibodies with distinct, non-overlapping epitopes may help maintain overall therapeutic efficacy.

Eliciting broadly cross-reactive antibody responses via vaccination, in combination with developing broadly protective therapeutic antibodies, may help reduce the likelihood that ongoing SARS-CoV-2 evolution and potential emerging sarbecoviruses will escape both existing protective immunity and available treatments. Indeed, broadly cross-reactive antibody responses have already been identified in patients vaccinated against SARS-CoV-2 following prior SARS-CoV-1 infection, indicating that it should be possible to elicit these responses in humans.^{32,33} Additionally, while boosting with WT SARS-CoV-2 protects against Omicron, protection may vary as other variants evolve; this underscores the need for a pan-sarbecovirus vaccine.^{2–4,14,15,34,35}

Efforts to focus the immune response to protective epitopes have extended to several different viruses, including influenza, HIV, respiratory syncytial virus (RSV), and SARS-CoV-2.^{25,36–38} Here, we used an immunogen design strategy to re-direct pre-existing antibody responses toward conserved epitopes by engineering putative N-linked glycosylation sites to “mask” undesirable epitopes.^{25,38} Immune re-focusing is particularly important in the context of immune imprinting to influence a memory-recall response that might otherwise be biased toward less conserved epitopes; such re-focusing can improve serum neutralization and protection. These immune imprinting and biased antibody responses were observed for SARS-CoV-2^{39–41} and parallel observations from influenza.^{42–44} Consequently, how to focus humoral immune responses toward broadly protective epitopes must be evaluated in context of pre-existing immunity. Our results show that human subjects generate cross-reactive antibodies targeting conserved epitopes and that these antibodies are genetically diverse. In mice, selectively boosting responses to one of these conserved epitopes using an engineered immunogen improved Omicron variant neutralization in the context of pre-existing immunity. Further experiments will be required to evaluate the impact of this immune focusing on protection, but these data provide proof of principle for an approach to pan-sarbecovirus vaccine design by demonstrating that prior knowledge of the exact variant or emerging sarbecovirus may not be required to elicit a broadly neutralizing antibody response.

LIMITATIONS OF THE STUDY

This study aims to provide proof-of-principle that focusing SARS-CoV-2 serum antibody responses to a conserved epitope in the context of SARS-CoV-2 spike imprinting can improve breadth. Further experiments, including *in vivo* protection studies, is necessary to establish whether this change is clinically meaningful. Additionally, RBD-directed antibodies represent only one possible class of broadly neutralizing antibodies. Antibodies targeting other conserved regions on the N-terminal domain or elsewhere on the spike glycoprotein could also confer protection, but these antibodies were not isolated in our sorting strategy. However, we note that most potently neutralizing monoclonal antibodies are RBD directed, making additional RBD-directed antibodies promising candidates to achieve broad neutralization.^{16,45–47}

STAR★METHODS

Detailed methods are provided in the online version of this paper and include the following:

- **KEY RESOURCES TABLE**
- **RESOURCE AVAILABILITY**
 - Lead contact
 - Materials availability
 - Data and code availability
- **EXPERIMENTAL MODEL AND SUBJECT DETAILS**
 - Human donor samples
 - Mice

- Cell lines

- **METHOD DETAILS**

- Immunogen and coronavirus protein expression and purification
- Probe generation
- Flow cytometry
- B cell receptor sequencing
- IgG expression and purification
- Serum and recombinant IgG ELISAs
- Competition ELISAs
- Competition biolayer interferometry
- Immunizations
- Pseudovirus neutralization assay
- Live virus neutralization assay

- **QUANTIFICATION AND STATISTICAL ANALYSIS**

SUPPLEMENTAL INFORMATION

Supplemental information can be found online at <https://doi.org/10.1016/j.xcrm.2022.100834>.

ACKNOWLEDGMENTS

We thank Dr. Jason McLellan from the University of Texas, Austin, for the spike plasmid. We thank Nir Hacohen and Michael Farzan for the kind gift of the ACE2-expressing 293T cells. We also thank Mark C. Poznansky and David J. Gregory from the Vaccine and Immunotherapy Center at Massachusetts General Hospital in Boston, MA, for developing the human donor sample protocol. We acknowledge funding from NIH R01s AI146779 (A.G.S.) and AI124378, AI137057, and AI153098 (D.L.), a Massachusetts Consortium on Pathogenesis Readiness (MassCPR) grant (A.G.S.), and training grants NIGMS T32 GM007753 and T32 GM144273 (B.M.H.); T32 AI007245 (J.F.); F31 AI138368 (M.S.); and F30 AI160908 (B.M.H.). A.B.B. is supported by the National Institute on Drug Abuse (NIDA) Avenir New Innovator Award DP2DA040254 and the MGH Transformative Scholars Program as well as funding from the Charles H. Hood Foundation (A.B.B.). This independent research was supported by the Gilead Sciences Research Scholars Program in HIV (A.B.B.). The BSL3 Laboratory where authentic virus work was performed is supported by Harvard CFAR (P30 AI060354) and MassCPR funding.

AUTHOR CONTRIBUTIONS

Conceptualization, B.M.H.; methodology, B.M.H., J.F., M.S., W.F.G.B., and A.G.S.; investigation, B.M.H., J.F., M.S., L.R., K.J.S., M.L.S., Y.C., J.B., I.W.W., A.C., M.V., M.R.C., T.K., and W.F.G.B.; writing – original draft, B.M.H. and A.G.S.; writing – review and editing, all authors; funding acquisition, A.B.B., D.L., W.F.G.B., and A.G.S.; supervision, A.B.B., D.L., W.F.G.B., and A.G.S.

DECLARATION OF INTERESTS

B.M.H. and A.G.S. have filed a provisional patent for the described immunogens.

Received: April 14, 2022

Revised: September 7, 2022

Accepted: November 8, 2022

Published: November 15, 2022

REFERENCES

1. Schmidt, F., Weisblum, Y., Rutkowska, M., Poston, D., DaSilva, J., Zhang, F., Bednarski, E., Cho, A., Schaefer-Babajew, D.J., Gaebler, C., et al. (2021). High genetic barrier to SARS-CoV-2 polyclonal neutralizing

- antibody escape. *Nature* 600, 512–516. <https://doi.org/10.1038/s41586-021-04005-0>.
2. van der Straten, K., Guerra, D., van Gils, M.J., Bontjer, I., Caniels, T.G., van Willigen, H.D.G., Wynberg, E., Poniman, M., Burger, J.A., Bouhuijs, J.H., et al. (2022). Mapping the antigenic diversification of SARS-CoV-2. Preprint at medRxiv. <https://doi.org/10.1101/2022.01.03.21268582>.
 3. Wilks, S.H., Mühlemann, B., Shen, X., Türel, S., LeGruesley, E.B., Netzl, A., Caniza, M.A., Chacaltana-Huarcaya, J.N., Daniell, X., Datto, M.B., et al. (2022). Mapping SARS-CoV-2 antigenic relationships and serological responses. Preprint at bioRxiv. <https://doi.org/10.1101/2022.01.28.477987>.
 4. Garcia-Beltran, W.F., St Denis, K.J., Hoelzemer, A., Lam, E.C., Nitido, A.D., Sheehan, M.L., Berrios, C., Ofoman, O., Chang, C.C., Hauser, B.M., et al. (2022). mRNA-based COVID-19 vaccine boosters induce neutralizing immunity against SARS-CoV-2 Omicron variant. *Cell* 185, 457–466.e4. <https://doi.org/10.1016/j.cell.2021.12.033>.
 5. Nabel, K.G., Clark, S.A., Shankar, S., Pan, J., Clark, L.E., Yang, P., Coscia, A., McKay, L.G.A., Varnum, H.H., Brusic, V., et al. (2022). Structural basis for continued antibody evasion by the SARS-CoV-2 receptor binding domain. *Science* 375, eabl6251. <https://doi.org/10.1126/science.abl6251>.
 6. Carreño, J.M., Alshammery, H., Tcheou, J., Singh, G., Raskin, A.J., Kawabata, H., Sominsky, L.A., Clark, J.J., Adelsberg, D.C., Bielak, D.A., et al. (2022). Activity of convalescent and vaccine serum against SARS-CoV-2 Omicron. *Nature* 602, 682–688. <https://doi.org/10.1038/s41586-022-04399-5>.
 7. Rössler, A., Riepler, L., Bante, D., von Laer, D., and Kimpel, J. (2022). SARS-CoV-2 omicron variant neutralization in serum from vaccinated and convalescent persons. *N. Engl. J. Med.* 386, 698–700. <https://doi.org/10.1056/NEJMc2119236>.
 8. Planas, D., Saunders, N., Maes, P., Guivel-Benhassine, F., Planchais, C., Buchrieser, J., Bolland, W.H., Porrot, F., Staropoli, I., Lemoine, F., et al. (2022). Considerable escape of SARS-CoV-2 Omicron to antibody neutralization. *Nature* 602, 671–675. <https://doi.org/10.1038/s41586-021-04389-z>.
 9. Menachery, V.D., Yount, B.L., Jr., Sims, A.C., Debink, K., Agnihothram, S.S., Gralinski, L.E., Graham, R.L., Scobey, T., Plante, J.A., Royal, S.R., et al. (2016). SARS-like WIV1-CoV poised for human emergence. *Proc. Natl. Acad. Sci. USA* 113, 3048–3053. <https://doi.org/10.1073/pnas.1517719113>.
 10. Menachery, V.D., Yount, B.L., Jr., Debink, K., Agnihothram, S., Gralinski, L.E., Plante, J.A., Graham, R.L., Scobey, T., Ge, X.Y., Donaldson, E.F., et al. (2015). A SARS-like cluster of circulating bat coronaviruses shows potential for human emergence. *Nat. Med.* 21, 1508–1513. <https://doi.org/10.1038/nm.3985>.
 11. Ge, X.Y., Li, J.L., Yang, X.L., Chmura, A.A., Zhu, G., Epstein, J.H., Mazet, J.K., Hu, B., Zhang, W., Peng, C., et al. (2013). Isolation and characterization of a bat SARS-like coronavirus that uses the ACE2 receptor. *Nature* 503, 535–538. <https://doi.org/10.1038/nature12711>.
 12. Starr, T.N., Zepeda, S.K., Walls, A.C., Greaney, A.J., Alkhovsky, S., Veessler, D., and Bloom, J.D. (2022). ACE2 binding is an ancestral and evolvable trait of sarbecoviruses. *Nature* 603, 913–918. <https://doi.org/10.1038/s41586-022-04464-z>.
 13. VanBlargan, L.A., Errico, J.M., Halfmann, P.J., Zost, S.J., Crowe, J.E., Jr., Purcell, L.A., Kawaoka, Y., Corti, D., Fremont, D.H., and Diamond, M.S. (2022). An infectious SARS-CoV-2 B.1.1.529 Omicron virus escapes neutralization by therapeutic monoclonal antibodies. *Nat. Med.* 28, 490–495. <https://doi.org/10.1038/s41591-021-01678-y>.
 14. Cao, Y., Wang, J., Jian, F., Xiao, T., Song, W., Yisimayi, A., Huang, W., Li, Q., Wang, P., An, R., et al. (2022). Omicron escapes the majority of existing SARS-CoV-2 neutralizing antibodies. *Nature* 602, 657–663. <https://doi.org/10.1038/s41586-021-04385-3>.
 15. Planas, D., Saunders, N., Maes, P., Guivel-Benhassine, F., Planchais, C., Buchrieser, J., Bolland, W.H., Porrot, F., Staropoli, I., Lemoine, F., et al. (2022). Considerable escape of SARS-CoV-2 Omicron to antibody neutralization. *Nature* 602, 671–675. <https://doi.org/10.1038/s41586-021-04389-z>.
 16. Rappazzo, C.G., Tse, L.V., Kaku, C.I., Wrapp, D., Sakharkar, M., Huang, D., Deveau, L.M., Yockachonis, T.J., Herbert, A.S., Battles, M.B., et al. (2021). Broad and potent activity against SARS-like viruses by an engineered human monoclonal antibody. *Science* 371, 823–829. <https://doi.org/10.1126/science.abf4830>.
 17. Robbiani, D.F., Gaebler, C., Muecksch, F., Lorenzi, J.C.C., Wang, Z., Cho, A., Agudelo, M., Barnes, C.O., Gazumyan, A., Finkin, S., et al. (2020). Convergent antibody responses to SARS-CoV-2 in convalescent individuals. *Nature* 584, 437–442. <https://doi.org/10.1038/s41586-020-2456-9>.
 18. Wang, Z., Schmidt, F., Weisblum, Y., Muecksch, F., Barnes, C.O., Finkin, S., Schaefer-Babajew, D., Cipolla, M., Gaebler, C., Lieberman, J.A., et al. (2021). mRNA vaccine-elicited antibodies to SARS-CoV-2 and circulating variants. Preprint at bioRxiv. <https://doi.org/10.1101/2021.01.15.426911>.
 19. Cho, A., Muecksch, F., Schaefer-Babajew, D., Wang, Z., Finkin, S., Gaebler, C., Ramos, V., Cipolla, M., Mendoza, P., Agudelo, M., et al. (2021). Anti-SARS-CoV-2 receptor-binding domain antibody evolution after mRNA vaccination. *Nature* 600, 517–522. <https://doi.org/10.1038/s41586-021-04060-7>.
 20. Barnes, C.O., Jette, C.A., Abernathy, M.E., Dam, K.M.A., Esswein, S.R., Gristick, H.B., Malyutin, A.G., Sharaf, N.G., Huey-Tubman, K.E., Lee, Y.E., et al. (2020). SARS-CoV-2 neutralizing antibody structures inform therapeutic strategies. *Nature* 588, 682–687. <https://doi.org/10.1038/s41586-020-2852-1>.
 21. Wu, Y., Wang, F., Shen, C., Peng, W., Li, D., Zhao, C., Li, Z., Li, S., Bi, Y., Yang, Y., et al. (2020). A noncompeting pair of human neutralizing antibodies block COVID-19 virus binding to its receptor ACE2. *Science* 368, 1274–1278. <https://doi.org/10.1126/science.abc2241>.
 22. Ju, B., Zhang, Q., Ge, J., Wang, R., Sun, J., Ge, X., Yu, J., Shan, S., Zhou, B., Song, S., et al. (2020). Human neutralizing antibodies elicited by SARS-CoV-2 infection. *Nature* 584, 115–119. <https://doi.org/10.1038/s41586-020-2380-z>.
 23. Yuan, M., Wu, N.C., Zhu, X., Lee, C.C.D., So, R.T.Y., Lv, H., Mok, C.K.P., and Wilson, I.A. (2020). A highly conserved cryptic epitope in the receptor binding domains of SARS-CoV-2 and SARS-CoV. *Science* 368, 630–633. <https://doi.org/10.1126/science.abb7269>.
 24. Wec, A.Z., Wrapp, D., Herbert, A.S., Maurer, D.P., Haslwanter, D., Sakharkar, M., Jangra, R.K., Dieterle, M.E., Lilov, A., Huang, D., et al. (2020). Broad neutralization of SARS-related viruses by human monoclonal antibodies. *Science* 369, 731–736. <https://doi.org/10.1126/science.abc7424>.
 25. Hauser, B.M., Sangesland, M., St Denis, K.J., Lam, E.C., Case, J.B., Windsor, I.W., Feldman, J., Caradonna, T.M., Kannegieter, T., Diamond, M.S., et al. (2022). Rationally designed immunogens enable immune focusing following SARS-CoV-2 spike imprinting. *Cell Rep.* 38, 110561. <https://doi.org/10.1016/j.celrep.2022.110561>.
 26. Tong, P., Gautam, A., Windsor, I.W., Travers, M., Chen, Y., Garcia, N., Whiteman, N.B., McKay, L.G.A., Storm, N., Malsick, L.E., et al. (2021). Memory B cell repertoire for recognition of evolving SARS-CoV-2 spike. *Cell* 184, 4969–4980.e15. <https://doi.org/10.1016/j.cell.2021.07.025>.
 27. Pinto, D., Park, Y.J., Beltramello, M., Walls, A.C., Tortorici, M.A., Bianchi, S., Jaconi, S., Culap, K., Zatta, F., De Marco, A., et al. (2020). Cross-neutralization of SARS-CoV-2 by a human monoclonal SARS-CoV antibody. *Nature* 583, 290–295. <https://doi.org/10.1038/s41586-020-2349-y>.
 28. Windsor, I.W., Tong, P., Lavidor, O., Moghaddam, A.S., McKay, L.G.A., Gautam, A., Chen, Y., MacDonald, E.A., Yoo, D.K., Griffiths, A., et al. (2022). Antibodies induced by ancestral SARS-CoV-2 strain that cross-neutralize variants from Alpha to Omicron BA.1. *Sci. Immunol.* 7, eabo3425. <https://doi.org/10.1126/sciimmunol.abo3425>.
 29. Liu, H., Wu, N.C., Yuan, M., Bangaru, S., Torres, J.L., Caniels, T.G., van Schooten, J., Zhu, X., Lee, C.C.D., Brouwer, P.J.M., et al. (2020). Cross-neutralization of a SARS-CoV-2 antibody to a functionally conserved site is mediated by avidity. *Immunity* 53, 1272–1280.e5. <https://doi.org/10.1016/j.immuni.2020.10.023>.
 30. Yin, W., Xu, Y., Xu, P., Cao, X., Wu, C., Gu, C., He, X., Wang, X., Huang, S., Yuan, Q., et al. (2022). Structures of the Omicron spike trimer with ACE2

- and an anti-Omicron antibody. *Science* 375, 1048–1053. <https://doi.org/10.1126/science.abn8863>.
31. Cameroni, E., Bowen, J.E., Rosen, L.E., Saliba, C., Zepeda, S.K., Culp, K., Pinto, D., VanBlargan, L.A., De Marco, A., di Iulio, J., et al. (2022). Broadly neutralizing antibodies overcome SARS-CoV-2 Omicron antigenic shift. *Nature* 602, 664–670. <https://doi.org/10.1038/s41586-021-04386-2>.
 32. Cao, Y., Yisimayi, A., Jian, F., Xiao, T., Song, W., Wang, J., Du, S., Zhang, Z., Liu, P., Hao, X., et al. (2022). Comprehensive epitope mapping of broad sarbecovirus neutralizing antibodies. Preprint at bioRxiv. <https://doi.org/10.1101/2022.02.07.479349>.
 33. Tan, C.W., Chia, W.N., Young, B.E., Zhu, F., Lim, B.L., Sia, W.R., Thein, T.L., Chen, M.I.C., Leo, Y.S., Lye, D.C., and Wang, L.F. (2021). Pan-sarbecovirus neutralizing antibodies in BNT162b2-immunized SARS-CoV-1 survivors. *N. Engl. J. Med.* 385, 1401–1406. <https://doi.org/10.1056/NEJMoa2108453>.
 34. Dejnirattisai, W., Huo, J., Zhou, D., Zahradnik, J., Supasa, P., Liu, C., Duyvesteyn, H.M.E., Ginn, H.M., Mentzer, A.J., Tuekprakhon, A., et al. (2022). SARS-CoV-2 Omicron-B.1.1.529 leads to widespread escape from neutralizing antibody responses. *Cell* 185, 467–484.e15. <https://doi.org/10.1016/j.cell.2021.12.046>.
 35. Cele, S., Jackson, L., Khoury, D.S., Khan, K., Moyo-Gwete, T., Tegally, H., San, J.E., Cromer, D., Scheepers, C., Amoako, D.G., et al. (2022). Omicron extensively but incompletely escapes Pfizer BNT162b2 neutralization. *Nature* 602, 654–656. <https://doi.org/10.1038/s41586-021-04387-1>.
 36. Correia, B.E., Bates, J.T., Loomis, R.J., Baneyx, G., Carrico, C., Jardine, J.G., Rupert, P., Correnti, C., Kalyuzhnyi, O., Vittal, V., et al. (2014). Proof of principle for epitope-focused vaccine design. *Nature* 507, 201–206. <https://doi.org/10.1038/nature12966>.
 37. Crispin, M., Ward, A.B., and Wilson, I.A. (2018). Structure and immune recognition of the HIV glycan shield. *Annu. Rev. Biophys.* 47, 499–523. <https://doi.org/10.1146/annurev-biophys-060414-034156>.
 38. Bajic, G., Maron, M.J., Adachi, Y., Onodera, T., McCarthy, K.R., McGee, C.E., Sempowski, G.D., Takahashi, Y., Kelsoe, G., Kuraoka, M., and Schmidt, A.G. (2019). Influenza antigen engineering focuses immune responses to a subdominant but broadly protective viral epitope. *Cell Host Microbe* 25, 827–835.e6. <https://doi.org/10.1016/j.chom.2019.04.003>.
 39. Aydilto, T., Rombauts, A., Stadlbauer, D., Aslam, S., Abelenda-Alonso, G., Escalera, A., Amanat, F., Jiang, K., Krammer, F., Carratala, J., and García-Sastre, A. (2021). Immunological imprinting of the antibody response in COVID-19 patients. *Nat. Commun.* 12, 3781. <https://doi.org/10.1038/s41467-021-23977-1>.
 40. Richardson, S.I., Madzorera, V.S., Spencer, H., Manamela, N.P., van der Mescht, M.A., Lambson, B.E., Oosthuysen, B., Ayres, F., Makhado, Z., Moyo-Gwete, T., et al. (2022). SARS-CoV-2 Omicron triggers cross-reactive neutralization and Fc effector functions in previously vaccinated, but not unvaccinated individuals. Preprint at medRxiv. <https://doi.org/10.1101/2022.02.10.22270789>.
 41. Röltgen, K., Nielsen, S.C.A., Silva, O., Younes, S.F., Zaslavsky, M., Costales, C., Yang, F., Wirz, O.F., Solis, D., Hoh, R.A., et al. (2022). Immune imprinting, breadth of variant recognition, and germinal center response in human SARS-CoV-2 infection and vaccination. *Cell* 185, 1025–1040.e14. <https://doi.org/10.1016/j.cell.2022.01.018>.
 42. Webster, R.G. (1966). Original antigenic sin in ferrets: the response to sequential infections with influenza viruses. *J. Immunol.* 97, 177–183.
 43. de St Groth, F., and Webster, R.G. (1966). Disquisitions of original antigenic sin. I. Evidence in man. *J. Exp. Med.* 124, 331–345. <https://doi.org/10.1084/jem.124.3.331>.
 44. Jensen, K.E., Davenport, F.M., Hennessy, A.V., and Francis, T., Jr. (1956). Characterization of influenza antibodies by serum absorption. *J. Exp. Med.* 104, 199–209. <https://doi.org/10.1084/jem.104.2.199>.
 45. Hansen, J., Baum, A., Pascal, K.E., Russo, V., Giordano, S., Wloga, E., Fulton, B.O., Yan, Y., Koon, K., Patel, K., et al. (2020). Studies in humanized mice and convalescent humans yield a SARS-CoV-2 antibody cocktail. *Science* 369, 1010–1014. <https://doi.org/10.1126/science.abd0827>.
 46. Greaney, A.J., Loes, A.N., Gentles, L.E., Crawford, K.H.D., Starr, T.N., Malone, K.D., Chu, H.Y., and Bloom, J.D. (2021). Antibodies elicited by mRNA-1273 vaccination bind more broadly to the receptor binding domain than do those from SARS-CoV-2 infection. *Sci. Transl. Med.* 13, eabi9915. <https://doi.org/10.1126/scitranslmed.abi9915>.
 47. Jones, B.E., Brown-Augsburger, P.L., Corbett, K.S., Westendorp, K., Davies, J., Cujec, T.P., Wiethoff, C.M., Blackbourne, J.L., Heinz, B.A., Foster, D., et al. (2021). The neutralizing antibody, LY-CoV555, protects against SARS-CoV-2 infection in nonhuman primates. *Sci. Transl. Med.* 13, eabf1906. <https://doi.org/10.1126/scitranslmed.abf1906>.
 48. Garcia-Beltran, W.F., Lam, E.C., St Denis, K., Nitido, A.D., Garcia, Z.H., Hauser, B.M., Feldman, J., Pavlovic, M.N., Gregory, D.J., Poznansky, M.C., et al. (2021). Multiple SARS-CoV-2 variants escape neutralization by vaccine-induced humoral immunity. *Cell* 184, 2372–2383.e9. <https://doi.org/10.1016/j.cell.2021.03.013>.
 49. Wrapp, D., Wang, N., Corbett, K.S., Goldsmith, J.A., Hsieh, C.L., Abiona, O., Graham, B.S., and McLellan, J.S. (2020). Cryo-EM structure of the 2019-nCoV spike in the prefusion conformation. *Science* 367, 1260–1263. <https://doi.org/10.1126/science.abb2507>.
 50. Moore, M.J., Dorfman, T., Li, W., Wong, S.K., Li, Y., Kuhn, J.H., Coderre, J., Vasilieva, N., Han, Z., Greenough, T.C., et al. (2004). Retroviruses pseudotyped with the severe acute respiratory syndrome coronavirus spike protein efficiently infect cells expressing angiotensin-converting enzyme 2. *J. Virol.* 78, 10628–10635. <https://doi.org/10.1128/JVI.78.19.10628-10635.2004>.
 51. Smith, K., Garman, L., Wrammert, J., Zheng, N.Y., Capra, J.D., Ahmed, R., and Wilson, P.C. (2009). Rapid generation of fully human monoclonal antibodies specific to a vaccinating antigen. *Nat. Protoc.* 4, 372–384. <https://doi.org/10.1038/nprot.2009.3>.
 52. Tiller, T., Meffre, E., Yurasov, S., Tsuiji, M., Nussenzweig, M.C., and Wardemann, H. (2008). Efficient generation of monoclonal antibodies from single human B cells by single cell RT-PCR and expression vector cloning. *J. Immunol. Methods* 329, 112–124. <https://doi.org/10.1016/j.jim.2007.09.017>.
 53. Slieden, K., van Montfort, T., Melchers, M., Isik, G., and Sanders, R.W. (2015). Immunosilencing a highly immunogenic protein trimerization domain. *J. Biol. Chem.* 290, 7436–7442. <https://doi.org/10.1074/jbc.M114.620534>.
 54. Schmidt, A.G., Do, K.T., McCarthy, K.R., Kepler, T.B., Liao, H.X., Moody, M.A., Haynes, B.F., and Harrison, S.C. (2015). Immunogenic stimulus for germ-line precursors of antibodies that engage the influenza hemagglutinin receptor-binding site. *Cell Rep.* 13, 2842–2850. <https://doi.org/10.1016/j.celrep.2015.11.063>.
 55. Schmidt, A.G., Therkelsen, M.D., Stewart, S., Kepler, T.B., Liao, H.X., Moody, M.A., Haynes, B.F., and Harrison, S.C. (2015). Viral receptor-binding site antibodies with diverse germline origins. *Cell* 161, 1026–1034. <https://doi.org/10.1016/j.cell.2015.04.028>.
 56. Garcia-Beltran, W.F., Lam, E.C., Astudillo, M.G., Yang, D., Miller, T.E., Feldman, J., Hauser, B.M., Caradonna, T.M., Clayton, K.L., Nitido, A.D., et al. (2021). COVID-19-neutralizing antibodies predict disease severity and survival. *Cell* 184, 476–488.e11. <https://doi.org/10.1016/j.cell.2020.12.015>.
 57. Siebring-van Olst, E., Vermeulen, C., de Menezes, R.X., Howell, M., Smit, E.F., and van Beusechem, V.W. (2013). Affordable luciferase reporter assay for cell-based high-throughput screening. *J. Biomol. Screen* 18, 453–461. <https://doi.org/10.1177/1087057112465184>.

STAR★METHODS

KEY RESOURCES TABLE

REAGENT or RESOURCE	SOURCE	IDENTIFIER
Antibodies		
CR3022	Produced in house ²³	N/A
S309	Produced in house ²⁷	N/A
P2B-2F6	Produced in house ²²	N/A
B38	Produced in house ²¹	N/A
ADI-55688	Produced in house ²⁴	N/A
Ab16	Produced in house ²⁵	N/A
HRP-conjugated rabbit anti-mouse IgG antibody	Abcam	CAT#ab97046; RRID: AB_10680920
HRP-conjugated goat anti-mouse IgG, human/bovine/horse SP ads antibody	Southern Biotech	CAT#1013-05
anti-human CD19-PE-Cy7	BioLegend	CAT#302216; RRID: AB_314246
anti-human CD3-APC-Cy7	BioLegend	CAT#317342; RRID: AB_2563410
anti-human IgG-BV711	BD Biosciences	CAT#564219; RRID: AB_2740459
anti-human IgD-PerCp-Cy5.5	BioLegend	CAT#348208; RRID: AB_10641706
anti-human IgM-BV605	BioLegend	CAT#314524; RRID: AB_2562374
anti-human CD27-PE Dazzle	BioLegend	CAT#356422; RRID: AB_2564101
anti-SARS-CoV-2 Nucleocapsid antibody	BioLegend	CAT#946102; RRID: AB_2892515
anti-mouse IgG1 PE-Cy7	BioLegend	CAT#406614; RRID: AB_2562002
Bacterial and virus strains		
Sarbecovirus pseudotyped viruses	Produced in house ⁴⁸	N/A
US-WA1/2020 ancestral variant of SARS-CoV-2	BEI Resources	Cat#NR-52281
Omicron BA.1 variant isolate	MassCPR Virus Repository	
Chemicals, peptides, and recombinant proteins		
Monomeric and trimeric SARS-CoV-2 receptor binding domains	Produced in house ²⁵	N/A
Monomeric SARS-CoV-1, WIV1, SHC014 and RaTG13 receptor binding domains	Produced in house ²⁵	N/A
SARS-CoV-2 two-proline stabilized spike ectodomain	Produced in house ⁴⁹	N/A
Hyperglycosylated (HG) SARS-CoV-2 trimer	This paper	N/A
Pierce HRV 3C protease	ThermoScientific	CAT#88946
Sigma Adjuvant System	SigmaAldrich	CAT#S6322
Streptavidin-PE conjugate	Invitrogen	CAT#12-4317-87
Aqua Live/Dead amine-reactive dye	ThermoFisher	CAT#L34957
Calcein, AM, cell-permeant dye	ThermoFisher	CAT#C3100MP
Streptavidin-BV421 conjugate	BioLegend	CAT#405225
Streptavidin-BV650 conjugate	BioLegend	CAT#405232
Streptavidin-APC conjugate	BioLegend	CAT#405207
RNaseOUT	ThermoFisher	CAT#10777019
TALON Metal Affinity Resin	Takara	CAT#635652
Pierce Protein G Agarose	ThermoFisher	CAT#20399
1-Step ABTS substrate	ThermoFisher	Prod#37615

(Continued on next page)

Continued

REAGENT or RESOURCE	SOURCE	IDENTIFIER
Critical commercial assays		
FAB2G Biosensors	ForteBio	Item#18-5125
SuperScript IV VILO MasterMix	ThermoFisher	CAT#11756050
Deposited data		
B cell receptor sequences	Mendeley; Genbank	https://doi.org/10.17632/4wmr6xb29g.1 ; see Table S4 (https://doi.org/10.17632/4wmr6xb29g.2) for Genbank accession numbers
Experimental models: Cell lines		
Human: Expi293F	Thermo Fisher	Cat#A14527; RRID: CVCL_D615
Human: A549-Ace2 cells	BEI Resources	Cat#NR-53821
Human: HEK 293T-humanACE2	Moore et al. ⁵⁰	N/A
Experimental models: Organisms/strains		
C57BL/6 mice (strain: C57BL/6NCrl)	Charles River Laboratories	Strain code: 027
Oligonucleotides		
Human B cell receptor sequencing primers	Smith et al. and Tiller et al. ^{51,52}	See Table S3 for oligo sequences
Software and algorithms		
FlowJo v10	TreeStar	https://www.flowjo.com ; RRID: SCR_008520
Prism v9	GraphPad	https://www.graphpad.com ; RRID: SCR_002798
IMGT	International ImMunoGeneTics Information System	http://www.imgt.org ; RRID: SCR_012780
Other		
Superdex 200 Increase 10/300 GL	GE Healthcare	Cytiva 28-9909-44

RESOURCE AVAILABILITY

Lead contact

Further information and requests for resources and reagents should be directed to and will be fulfilled by the lead contact, Aaron G. Schmidt (aschmidt@crystal.harvard.edu).

Materials availability

All unique/stable reagents generated in this study will be made available on request, but we may require a payment and/or a completed materials transfer agreement if there is potential for commercial application. For non-commercial use, all unique/stable reagents generated in this study are available from the [lead contact](#) with a completed materials transfer agreement.

Data and code availability

- B cell receptor sequences have been deposited in Genbank. Accession numbers are listed in Table S4. B cell receptor sequences are also available from Mendeley Data at <https://doi.org/10.17632/4wmr6xb29g.1>.
- This paper does not report original code.
- Any additional information required to reanalyze the data reported in this paper is available from the [lead contact](#) upon request.

EXPERIMENTAL MODEL AND SUBJECT DETAILS

Human donor samples

Human peripheral blood mononuclear cells were isolated for cell sorting from samples previously published⁴; samples were obtained with approval from the Partners Institutional Review Board (protocol 2020P002274). All measurements relating to donor samples were obtained from separate samples, rather than repeated measurements of the same samples. Table S1 contains all available data about these 10 donors; all other demographic data are unavailable.

Mice

All immunizations were performed using female C57BL/6 mice (Charles River Laboratories, strain 027) aged 6–10 weeks. Immunization experiments were conducted with institutional IACUC approval (MGH protocol 2014N000252).

Cell lines

Expi293F cells (Thermo Fisher Cat#A14527; RRID: CVCL_D615) cells were cultured in accordance with the manufacturer's instructions. Human ACE2 expressing HEK 293T cells⁵⁰ were a gift from Nir Hacohen and Michael Farzan and were cultured in Dulbecco's Modified Eagle Medium (ThermoFisher) with 2% fetal bovine serum (Peak Serum FBS) and 1% penicillin-streptomycin at 10,000 U/mL (Gibco). A549-Ace2 cells (BEI Resources, Cat # NR-53821) were cultured in in D10+ media (DMEM (Corning) supplemented with HEPES (Corning), 1X Penicillin 100 IU/mL/Streptomycin 100 µg/mL (Corning), 1X Glutamine (Glutamax, ThermoFisher Scientific), and 10% Fetal Bovine serum (FBS; Sigma).

METHOD DETAILS

Immunogen and coronavirus protein expression and purification

Coronavirus receptor binding domains (RBDs) were based on the following Genbank sequences: SARS-CoV-2 RBD (Genbank MN975262.1), SARS-CoV-1 RBD (Genbank)ABD72970.1, WIV1 RBD (Genbank AGZ48828.1), RaTG13 RBD (Genbank QHR63300.2), SHC014 RBD (Genbank QJE50589.1). All constructs were purchased as gblocks following codon optimization using Integrated DNA Technologies. Genes were cloned into pVRC and sequence confirmed via Genewiz. Monomeric constructs used for ELISA coating and single B cell sorting included C-terminal HRV 3C-cleavable 8xHis and Avi tags, and trimeric constructs included a C-terminal HRV 3C-cleavable 8xHis tag and a hyperglycosylated GCN4 tag with two engineered C-terminal cystines, the lattermost tag being derived from a previously published hyperglycosylated GCN4 tag.⁵³ The spike plasmid was provided courtesy of Dr. Jason McLellan at the University of Texas, Austin, containing C-terminal HRV 3C cleavable 6xHis and 2xStrep II tags and a non-cleavable foldon trimerization domain.⁴⁹

Proteins were expressed in Expi293F cells (ThermoFisher) after transfection using Expifectamine per manufacturer's protocol. After 7 days, transfections were harvested and centrifuged for clarification. Immobilized metal-affinity chromatography using Cobalt-TALON resin (Takara) was performed via the 8xHis tag. Proteins were eluted with 350 mM imidazole, concentrated, and passed over a size exclusion column (Superdex 200 Increase 10/300 GL, GE Healthcare) in PBS (Corning). Affinity tags were cleaved by HRV 3C protease (ThermoScientific) and purified protein was isolated by orthogonal purification using Cobalt-TALON resin to remove the His-tagged HRV 3C protease, cleaved tag, and uncleaved protein.

Probe generation

Site-specific biotinylation of Avi-tagged coronavirus RBDs was performed using a BirA biotin-protein ligase reaction kit (Avidity) according to manufacturer's protocol. Proteins were re-purified using the size exclusion column (Superdex 200 Increase 10/300 GL, GE Healthcare) in PBS (Corning). Streptavidin conjugates were added to a final conjugated probe concentration of 0.1 µg/mL with a final molar ratio of probe to streptavidin valency of 1:1. Probes were incubated at 4°C for at least one hour prior to being used to label cells.

Flow cytometry

Human peripheral blood mononuclear cells for cell sorting were stained with the following coronavirus RBD probes at a final concentration of 25 nM each: wild-type SARS-CoV-2-PE (streptavidin-PE from Invitrogen), Omicron-APC (streptavidin-APC from BioLegend), SARS-CoV-1-BV650 (streptavidin-BV650 from BioLegend), SHC014-BV421 (streptavidin-BV421 from BioLegend); labelling occurred at 4°C for 30 minutes. A mixture of anti-human antibodies at 25 nM was then added: anti-human CD19-PE-Cy7 (BioLegend), anti-human CD3-APC-Cy7 (BioLegend), anti-human IgG-BV711 (BD Biosciences), anti-human IgD-PerCp-Cy5.5 (BioLegend), anti-human IgM-BV605 (BioLegend), anti-human CD27-PE Dazzle (BioLegend); labelling occurred for 30 minutes at 4°C. Cells were then washed twice with PBS and labelled with near-IR live/dead stain (ThermoFisher) for 15 minutes at 4°C. Cells were then washed twice with PBS prior to flow cytometry. Flow cytometry was run on a BD FACSAria Fusion cytometer (BD Biosciences), using FlowJo (version 10) for data analysis.

B cell receptor sequencing

96-well plates were prepared with 4 µL of lysis buffer (0.5X PBS, 10 mM DTT, 4 units of ThermoFisher RNaseOUT). Cells were sorted and centrifuged at 3000 RCF for 1 minute and stored at –80°C. After later thawing, a reverse transcriptase reaction was performed by adding 20 µL of SuperScript IV VILO MasterMix (ThermoFisher). Previously published primers^{51,52} were used to perform two cycles of PCR with Herculase II Fusion DNA polymerase (Agilent) before submission to Genewiz for Sanger sequencing of variable heavy and light chains. Sequences were analyzed using IMGT High V-Quest.

IgG expression and purification

Variable heavy and light chain genes were synthesized as gBlocks from Integrated DNA Technologies and cloned into pVRC plasmids containing appropriate constant domains.^{54,55} Fabs and IgGs were purified and transfected using the same protocol for

immunogens and coating proteins. The heavy chain plasmid included a HRV 3C-cleavable 8xHis tag, and the IgG heavy chain vector included HRV 3C-cleavable 8xHis tags.

Serum and recombinant IgG ELISAs

Serum ELISAs were done using Corning clear flat-bottom 96-well high binding microplates. Plates were coated with protein a concentration of 2.5 $\mu\text{g}/\text{mL}$ (in PBS) at a working volume of 100 μL , then incubated overnight (>8 hours) at 4°C. Following incubation, coating solution was decanted, and all wells were blocked with 150 μL of 1% BSA in PBS with 1% Tween for 120 minutes at ambient temperature. After blocking, sera diluted 40-fold or IgGs at a specified concentration were prepared as primary antibody solution, then serially diluted 5-fold in tubes. For serum ELISAs, CR3022 IgG was also serially diluted (5-fold) from a 5 $\mu\text{g}/\text{mL}$ starting concentration, to serve as a control curve. 40 μL of primary antibody solution was then added to each well, and plates were incubated at ambient temperature for 90 minutes. After incubation, plates were washed three times in PBS/Tween solution.

The secondary antibody solution consisted of Abcam HRP-conjugated rabbit anti-mouse IgG antibody (for mouse serum ELISAs) or Abcam HRP-conjugated goat anti-human IgG antibody (for human IgG ELISAs) diluted 1:20,000 in PBS. 150 μL of the resulting solution was added to each well before incubating for one hour at ambient temperature. Plates were again washed three times with PBS/Tween solution. Following manufacturer (ThermoFisher) protocol, 150 μL of 1xABTS development solution was added to each well for color development, which was arrested after 30 minutes with 100 μL of 0.1% sodium azide. Plates were read using a SpectraMaxiD3 plate reader (Molecular Devices) for absorbance at 405 nm.

Competition ELISAs

Competition ELISAs were performed as previously described.²⁶ Corning clear flat-bottom 96-well high binding microplates were coated with wild-type SARS-CoV-2 RBD at 2.5 $\mu\text{g}/\text{mL}$ (in PBS) overnight (>8 hours) at 4°C. Coating solution was removed, and plates were blocked with PBS-Tween with 4% BSA for 120 minutes. Relevant IgGs were coated onto the plate at a concentration of 0.2 mg/mL using a working volume of 25 μL . An equivalent volume of biotinylated IgG was then added at a concentration of 0.2 $\mu\text{g}/\text{mL}$ and incubated for 90 minutes at ambient temperature. Primary solution was decanted and plates were washed 3x with PBS/Tween buffer solution. 150 μL of HRP-conjugated streptavidin (ThermoFisher) was then incubated at a concentration of 1:5000 for secondary incubation of 1 hour. After this point, the protocol was identical to the serum ELISA method for steps beyond secondary incubation. A no-competition control was used for comparison to assess binding loss from competition, and percent loss was computed relative to this control; graphs of data including negative percent binding loss represent the loss as 0%.

Competition biolayer interferometry

Antibody competition with D2G2 (a representative of the group of antibodies that does not target a class 4 epitope) was assessed via biolayer interferometry (BLI). SARS-CoV-2 RBD at 8 μM was complexed with at least a 5-molar excess of Fab for 30 minutes. Binding of the complex to D2G2 Fab was measured using a BLItz (ForteBio). Ni-NTA sensors (Sartorius) were used with D2G2 immobilized and complexes as the analytes. Absorbance was recorded and used to qualitatively assess whether D2G2 was able to bind to the complex. All reagents were diluted in 1X Kinetics Buffer (ForteBio).

Antibody competition with Ab16 (a class 4 antibody) was also assessed via BLI. SARS-CoV-2 RBD at 8 μM was complexed with at least a 5-molar excess Ab16 Fab for 30 minutes, and then binding of the complex to the B3E3, B8E8, and D2G2 Fabs was measured using a BLItz (ForteBio) and compared to binding of SARS-CoV-2 RBD at 8 μM without Ab16 to qualitatively determine whether each Fab was able to bind the SARS-CoV-2 RBD:Ab16 complex. FAB2G sensors were used with B3E3, B8E8, or D2G2 immobilized and SARS-CoV-2 RBD:Ab16 complexes or SARS-CoV-2 RBD as the analytes. All reagents were diluted in 1X Kinetics Buffer (ForteBio).

Immunizations

Female C57BL/6 mice (Charles River Laboratories) aged 6–10 weeks were used for all immunizations. Mice were immunized by the intraperitoneal route, introducing 20 μg of protein adjuvanted with 50% w/v Sigma adjuvant per 100 μL of inoculum. Priming occurred on day –21, boosts occurred at days 0 and 21, and serum was collected on day 35 from all cohorts. Two separate replicates of the immunization experiments were performed, the first with N = 5 mice per cohort and the second with N = 10 mice per cohort. All immunizations were approved by institutional IACUC (MGH protocol 2014N000252).

Pseudovirus neutralization assay

Monoclonal IgGs and mouse sera were assayed against wild-type SARS-CoV-2, Omicron variant SARS-CoV-2, Delta variant SARS-CoV-2, SARS-CoV-1, WIV1, RaTG13, and SHC014 pseudotyped lentiviral particles expressing spike proteins described previously.⁵⁶ Lentiviral particles were generated via transient transfection of 293T cells, with viral supernatant titers assessed via flow cytometry of 293T-ACE2 cells⁵⁰ and the HIV-1 p24^{CA} antigen capture assay (Leidos Biomedical Research, Inc.). All assays were performed in a 384-well format (plates from Grenier) using a Tecan Fluent Automated Workstation.

Mouse serum samples started at an initial 1:3 dilution followed by six subsequent serial 3-fold dilutions. Monoclonal IgGs started at an initial specified concentration and then were subsequently diluted 3-fold as well. Each plate well contained 20 μL of sera and 20 μL of pseudovirus (125 infectious units); this mixture was incubated for 1 hour at room temperature. 10,000 293T-ACE2 cells⁵⁰ in 20 μL of media containing 15 $\mu\text{g}/\text{mL}$ polybrene was then added to each well and incubated at 37°C for an additional 60–72 hours.

Assay buffers described previously⁵⁷ were used to perform cell lysis, and luciferase expression was then measured with a Spectramax L luminometer (Molecular Devices). Background luminescence from cells-only sample wells was calculated and subtracted from each sample well. Neutralization percentage at a given serum or monoclonal IgG concentration was then calculated by dividing by the luminescence of wells containing only virus and cells. GraphPad Prism (version 9) was used to fit nonlinear regressions to the data and used to calculate IC₅₀ values for all serum samples with neutralization values greater than or equal to 80% at maximum concentration. NT₅₀ values were then calculated by taking the reciprocal of the IC₅₀ values.

Live virus neutralization assay

The live virus neutralization assays were carried out in the Biosafety Level 3 laboratory of the Ragon Institute of MGH, MIT, and Harvard.

A549-Ace2 cells (BEI Resources, Cat # NR-53821) were cultured in D10+ media (DMEM (Corning) supplemented with HEPES (Corning), 1X Penicillin 100 IU/mL/Streptomycin 100 µg/mL (Corning), 1X Glutamine (Glutamax, ThermoFisher Scientific), and 10% Fetal Bovine serum (FBS; Sigma). The cells were detached using Trypsin-EDTA (Fisher Scientific) and seeded at 40,000 cells per well in 96-well plates 16–20 hours before infection. 4 hours before the infection, the cell culture supernatant was removed and 75 µL of D2+ media was added (2% FBS instead of 10%).

The US-WA1/2020 ancestral variant of SARS-CoV-2 was obtained from BEI Resources (Cat # NR-52281). The Omicron BA.1 variant isolate was obtained from the MassCPR variant repository. In brief, the variant had previously been isolated in the Ragon Institute BSL3 by rescue on Vero-E6 cells (ATCC) from primary clinical specimens, and it was then contributed to the MassCPR variant repository. The sequence of all viral stocks was confirmed by whole genome sequencing to ensure that no additional mutation arose during virus expansion. In-house prepared viral stocks (US-WA1/2020 Passage 3 and omicron BA.1 Passage 1) were diluted in D+ media to 32,000 pfu/mL to achieve a multiplicity of infection of 0.01 when added to the cells in the 96-well plates.

The antibody stocks (1 mg/mL) were diluted in D+ media (DMEM supplemented with HEPES, 1X Penicillin 100 IU/mL/Streptomycin 100 mg/mL and 1X Glutamine) to 2x desired final concentration by 3-fold serial dilutions. Equal volumes of viral stock and antibody dilution solutions were mixed and incubated for 1 hour at 37°C at 5% CO₂. After the incubation, for each condition, 25 µL of virus-antibody solutions (or no antibody control) were added to triplicate wells in 96-well plates. The plates were then spininfected at 2,000 x g for 30 minutes at 37°C followed by a 48-hour incubation at 37°C at 5% CO₂.

After 48 hours, the cell culture supernatant was discarded, the cells were washed with PBS (Corning) then harvested using TrypLE (Life Technologies) and D10+ media before being transferred to a V-bottom 96-well plate for flow cytometry staining. Cells were washed in PBS, then stained with live/dead fixable blue stain (Thermo Fisher) for 30 minutes at 4°C. Cells were then washed in flow cytometry buffer (2% FBS in PBS) and fixed using 4% paraformaldehyde (Santa Cruz) for 30 minutes at 4°C. The fixed cells were removed from the BSL3 laboratory and prepared for intracellular staining using Perm/Wash buffer (BD Biosciences). The permeabilized cells were stained with mouse anti-SARS-CoV-2 Nucleocapsid antibody (Biolegend) for 30 minutes at 4°C, then washed and stained with secondary antibody labelled with PE-Cy7 (Biolegend) for 30 minutes at 4°C. Finally, the cells were washed and re-suspended in flow cytometry buffer. Flow cytometry was performed on a BD Symphony (BD Biosciences).

QUANTIFICATION AND STATISTICAL ANALYSIS

All FCS files generated from flow cytometry were analyzed using FlowJo software (version 10). GraphPad Prism (version 9) was used to fit asymmetric 4PL curves to the neutralization data which were used to calculate IC₅₀ and NT₅₀ values. GraphPad Prism was also used to perform other statistical analyses: the Kruskal-Wallis non-parametric ANOVA with post hoc analysis using Dunn's test for multiple comparisons was used to compare multiple populations, and the Mann-Whitney U test was used to compare two populations without consideration of paired samples. A p value < 0.05 was considered to be statistically significant.